



Swansea University
Prifysgol Abertawe



Cronfa - Swansea University Open Access Repository

This is an author produced version of a paper published in:
IEEE Transactions on Power Delivery

Cronfa URL for this paper:
<http://cronfa.swan.ac.uk/Record/cronfa44927>

Paper:

Furlani Bastos, A., Lao, K., Todeschini, G. & Santoso, S. (2018). Accurate Identification of Point-on-Wave Inception and Recovery Instants of Voltage Sags and Swells. *IEEE Transactions on Power Delivery*, 1-1.
<http://dx.doi.org/10.1109/TPWRD.2018.2876682>

This item is brought to you by Swansea University. Any person downloading material is agreeing to abide by the terms of the repository licence. Copies of full text items may be used or reproduced in any format or medium, without prior permission for personal research or study, educational or non-commercial purposes only. The copyright for any work remains with the original author unless otherwise specified. The full-text must not be sold in any format or medium without the formal permission of the copyright holder.

Permission for multiple reproductions should be obtained from the original author.

Authors are personally responsible for adhering to copyright and publisher restrictions when uploading content to the repository.

<http://www.swansea.ac.uk/library/researchsupport/ris-support/>

Accurate Identification of Point-on-Wave Inception and Recovery Instants of Voltage Sags and Swells

Alvaro Furlani Bastos, *Student Member, IEEE*, Keng-Weng Lao, *Member, IEEE*,
Grazia Todeschini, *Senior Member, IEEE*, and Surya Santoso, *Fellow, IEEE*

Abstract—Voltage sags and swells are power quality events commonly observed in power systems; however, none of the existing methods allows determining their point-on-wave inception and recovery instants (and consequently, their duration) accurately in all cases. The primary goal of this paper is to determine these instants with little or no delay, by calculating the absolute rms voltage difference between two adjacent sliding windows. The proposed method is based on the assumption that this difference is maximum when the sample under analysis corresponds to either the inception or the recovery instant. This method is valid for both sag and swell events, with or without transients. Evaluation of the proposed method performance for different types of events shows that it is robust and highly accurate in determining the inception and recovery instants. The estimation error for the majority of the events analyzed is either 0 or 1 sample (each sample corresponds to a phase-angle difference of 2.81°), while the worst performance is 3 samples.

Index Terms—inception instant, point-on-wave, recovery instant, voltage sag, voltage swell

I. INTRODUCTION

INDUSTRY standards recommend to characterize a voltage variation event on the basis of its duration and minimum (or maximum) rms voltage during the sag (or swell) [1], [2]. Other event characteristics, such as point-on-wave inception and recovery instants, and phase shift, are commonly not included in the event characterization. Due to the unavailability of these parameters, industry standards recommend not considering them for the evaluation of equipment sensitivity against voltage sags and swells [3], [4].

Some studies have shown that sensitivity of equipment is influenced by sag/swell characteristics other than duration and magnitude. For example, [5] reports that the sensitivity of relays, motor-starters, and contactors for voltage sags shorter than 4-5 cycles is highest for 90° point-on-wave inception. On the other hand, higher sensitivity is observed for 0° point-on-wave inception for sags longer than 5 cycles. Additionally,

A. F. Bastos is with the Department of Electrical and Computer Engineering, The University of Texas at Austin, Austin TX 78712 USA, and also with the CAPES Foundation within the Ministry of Education, Brasilia 70040-031, Brazil (e-mail: alvaro.fbastos@utexas.edu).

K.-W. Lao is with the Department of Electrical and Computer Engineering, University of Macau, Macao 999078, China, and also with the Department of Electrical and Computer Engineering, The University of Texas at Austin, Austin, TX 78712 USA (e-mail: johnnylao@umac.mo).

G. Todeschini is with the College of Engineering, Swansea University, Swansea SA1 8EN, U.K. (e-mail: grazia.todeschini@swansea.ac.uk).

S. Santoso is with the Department of Electrical and Computer Engineering, The University of Texas at Austin, Austin TX 78712 USA (e-mail: ssantoso@mail.utexas.edu).

calculation of reliability indices requires an accurate estimate of the duration of voltage variation events [1].

Many methods have been developed to identify and characterize voltage sags/swells, such as threshold rms voltage [1], [2], [6], [7], waveform envelope [5], [8], discrete wavelet transform [9]–[13], missing voltage [14]–[16], dq transformation [17], [18], numerical matrix [18], and peak detector [19]–[21]. The existing approaches use either instantaneous or rms measurements of single or three-phase voltage waveforms. Some of them provide information about the residual voltage magnitude during the event. However, none of these methods provide accurate estimates for the point-on-wave inception and recovery instants for all types of sags/swells. For example, the threshold rms voltage method introduces an error up to 1 cycle in the estimation of the inception and recovery instants, while the discrete wavelet transform method performs well only if the voltage variation event is accompanied by transients [22].

This paper proposes a method to accurately determine the point-on-wave inception and recovery instants of voltage sags and swells. Initially, the traditional threshold rms voltage method recommended by industry standards and its limitations are discussed in Section II. The novel method presented in this paper aims at overcoming those limitations, and it is based on the absolute difference between rms voltage values of sliding windows, as described in Section III. The performance of this method is assessed in Section IV, where it is shown that the method is robust and performs well for a wide class of sag and swell events.

II. MOTIVATION - THE TRADITIONAL METHOD

The procedure given in industrial standards to characterize a voltage sag or swell is based on the rms voltage profile [1], [2]. The rms voltage value at instant k , $V_{rms}[k]$, is calculated from the sampled instantaneous voltage values, $v[k]$, over an one-cycle long sliding window, as shown in (1):

$$V_{rms}[k] = \sqrt{\frac{1}{N} \sum_{p=k-N+1}^k v[p]^2} \quad (1)$$

where N is the number of samples per cycle. The rms voltage values are updated every half-cycle, and therefore the subsequent values are computed at indices $(k + h\frac{N}{2})$, where h is an integer number. The time resolution of the resulting discrete time sequence is half-cycle.

A voltage sag (or swell) is detected if the computed rms voltage drops below (or rises above) a pre-specified threshold value, α_{inf} (or α_{sup}), where the rms voltage values are given

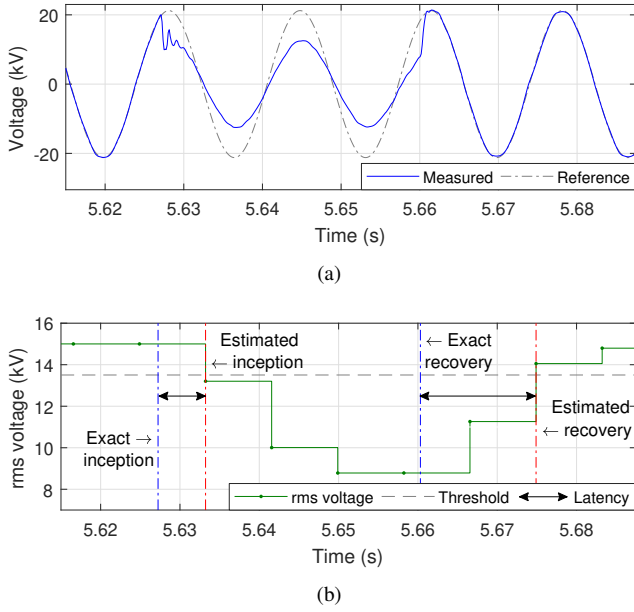


Fig. 1. Illustration of the time latency introduced by the traditional method in determining the inception and recovery instants of a voltage sag. (a) Voltage waveform. (b) rms voltage profile (time resolution of half-cycle).

in pu. This method will be referred to as *traditional method* in the remaining of this paper. In spite of being widely used, this method is not accurate in determining the inception and recovery instants of the voltage variation event. The rms operator produces an averaging effect, and as a result, the rms voltage profile may take up to one cycle to reach a new steady-state value after the event inception or recovery [6]. This behavior can be improved by decreasing the interval between consecutive rms computations; the best scenario occurs when rms voltage values are updated for every new sample of the instantaneous voltage waveform.

Consider that a sag/swell starts at instant k_1 ; thus, all sliding windows used to compute the rms voltage values from k_1 to $(k_1 + N - 1)$ contain both pre-event and during-event voltage samples. This portion of the rms voltage profile is denominated *transition segment* and contains data between two quasi-stationary segments [7].

The maximum duration of a transition segment depends on the length of the rms sliding window and the time resolution of the rms voltage profile. Using (1) with a time resolution of one sample, the rms voltage profile gradually changes from $V_{rms}[k_1 - 1]$ to $V_{rms}[k_1 + N]$, even for voltage variation events with a rectangular shape. The slope of this change is proportional to the difference of the voltage levels immediately before and after the disturbance inception. Therefore, the transition segment lasts one cycle and the estimated inception point is located within the interval $[k_1 - 1 : k_1 + N]$. The time delay between the exact inception instant and the estimated one is referred to as *time latency*. The worst case occurs when the sag magnitude is minimum, i.e. $(1 - \alpha_{inf})$; in such case, the rms voltage profile reaches α_{inf} only at $(k_1 + N)$ and the time latency is equal to one cycle. A similar effect is observed in estimating the recovery instant.

As an illustration, Fig. 1a represents the voltage waveform

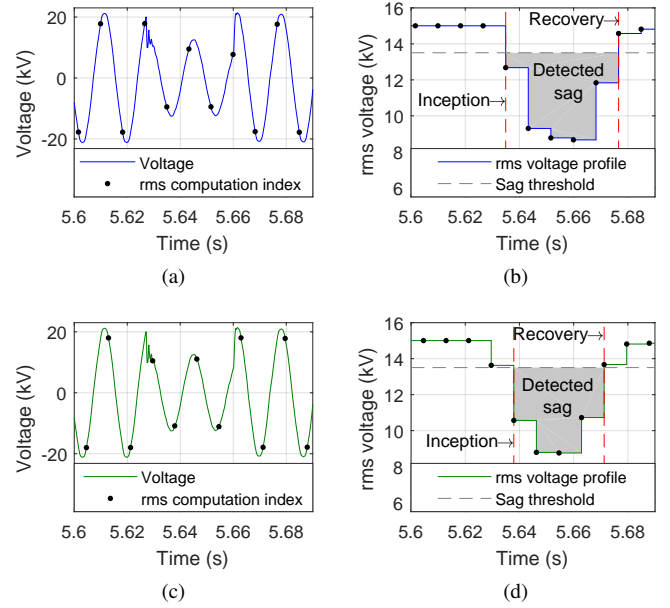


Fig. 2. Illustration of the inaccuracy in determining the sag duration and retained voltage according to the traditional method. Each black dot represents the instants at which rms values are updated. (a)-(b) Case 1. (c)-(d) Case 2.

during a sag event, while Fig. 1b shows the corresponding rms voltage profile, computed according to (1). The exact inception and recovery instants are determined by visual inspection of the measured and reference voltage waveforms. On the other hand, the inception and recovery instants estimated by the traditional threshold rms method (adopting $\alpha_{inf} = 0.9$ pu) are not accurate. The time latencies are 0.359 and 0.875 cycle, respectively; such large inaccuracies prevent the use of the estimated point-on-wave inception and recovery values in equipment sensitivity analysis. The lowest time latency for the traditional method is obtained through short sliding windows (half-cycle) and high update rate (rms values computed for each new voltage sample). However, even this approach has been shown to introduce a relatively high time latency [22].

Additionally, the estimated event duration depends on the instants at which the rms values are computed. Industry standards state that “the duration [of a voltage sag] is the time that the rms voltage stays below the threshold” [1]. Fig. 2 shows two rms voltage profiles for the same sag event, where the rms values are calculated at different instants. It can be observed that the event duration is not uniquely established under this definition, and the estimated inception and recovery instants are different in each case. The estimated event duration values are 2.502 cycles for case 1 and 1.998 cycles for case 2. This result is of concern because the difference between the two event durations (0.504 cycle) is sufficiently large to change the classification of a disturbance from ‘instantaneous short-duration variation’ to ‘non-event’ or vice versa [23].

Furthermore, the value of the retained voltage is affected by the rms update instants [7]. The two values obtained for the sag represented in Fig. 2 are 8.68 kV and 8.76 kV, respectively. More in general, for sag durations shorter than 1.5 cycles, the value of the retained voltage calculated with the traditional

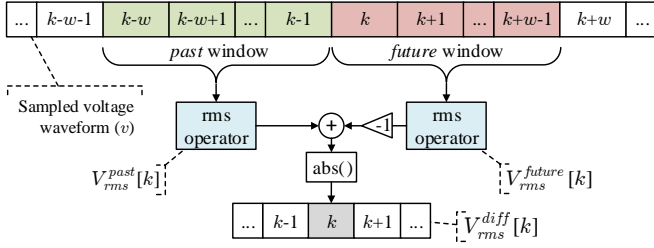


Fig. 3. Computation of the values of V_{rms}^{past} , V_{rms}^{future} , and V_{rms}^{diff} at instant k for a given sampled voltage waveform.

method is likely to be inaccurate. This is explained as follows: for short sags, the sliding window does not contain exclusively voltage samples measured during the event, and therefore the rms calculation is affected by pre-event or post-event values. Similar considerations apply to voltage swells.

III. RMS VOLTAGE DIFFERENCE ESTIMATION METHOD

A. The rms Voltage Difference Profile

The method proposed in this paper aims at accurately determining the inception and recovery instants of a voltage variation event, as well as the amplitude variation. To reach these aims, two new quantities based on the traditional rms definition are proposed in (2):

$$V_{rms}^{past}[k] = \sqrt{\frac{1}{w} \sum_{p=k-w}^{k-1} v[p]^2} \quad (2)$$

$$V_{rms}^{future}[k] = \sqrt{\frac{1}{w} \sum_{p=k}^{k+w-1} v[p]^2}$$

where w is the sliding window length, and k is the time index under analysis. These quantities are calculated through two sliding windows: the *past* window, ranging from $(k-w)$ to $(k-1)$, and the *future* window, ranging from k to $(k+w-1)$. These definitions are introduced such that the rms voltage values at the inception and recovery instants are affected by exclusively pre-, during-, or post-event instantaneous voltage samples. As a result, the rms voltage profile will exhibit a sharp transition at the event inception and recovery instants – rather than a gradual one, as in the traditional method. Therefore, these instants could be determined accurately. A related idea using two adjacent, non-overlapping sliding windows is discussed in [24], [25] for a signal segmentation scheme.

The estimation of the inception and recovery instants of the voltage variation event is based on the absolute difference between *past* and *future* rms voltage values, defined in (3). Fig. 3 illustrates the computation of the V_{rms}^{diff} profile according to this definition.

$$V_{rms}^{diff}[k] = |V_{rms}^{past}[k] - V_{rms}^{future}[k]| \quad (3)$$

The underlying reasoning of this method is that there are only three possible cases for the voltage samples within each sliding window: (1) exclusively pre- or post-event data, (2) exclusively during-event data, or (3) a combination of both. If both *past* and *future* windows contain exclusively pre-event

data, then the quantity V_{rms}^{diff} is close to zero; the same is true for exclusively post- or during-event data. On the other hand, V_{rms}^{diff} increases as the *past* and *future* windows move through the voltage signal and one of them covers both event and non-event data. At the inception (recovery) instant, the *past* window contains exclusively pre-event (during-event) samples, while the *future* window contains exclusively during-event (post-event) samples. In this case, V_{rms}^{diff} reaches its maximum value; for a voltage variation event with rectangular shape, this maximum value corresponds to the sag/swell magnitude.

The claim that V_{rms}^{diff} reaches its maximum value at the inception and recovery instants of a voltage variation event is demonstrated through the simple case of a sinusoidal voltage waveform. For simplicity, only the inception instant is examined, as the discussion for the recovery instant is analogous. Consider that the instantaneous sampled voltage, $v[k]$, is modeled as in (4), where k^* corresponds to the inception instant of a sag event.

$$v[k] = \begin{cases} v_1[k] := V_1 \sin(2\pi f k + \phi), & \text{if } k < k^* \\ v_2[k] := V_2 \sin(2\pi f k + \phi), & \text{if } k \geq k^* \end{cases} \quad (4)$$

where V_1 and V_2 are the magnitudes before and during the voltage sag, respectively; f and ϕ are the frequency and phase angle, respectively. The V_{rms}^{diff} profile as function of time for a voltage sag longer than w samples is shown in (5).

$$V_{rms}^{diff}[k] = \begin{cases} 0, & \text{if } k \leq (k^* - w) & (5a) \\ \frac{V_1}{\sqrt{2}} - V_{bf}[k], & \text{if } (k^* - w) < k < k^* & (5b) \\ \frac{V_1 - V_2}{\sqrt{2}}, & \text{if } k = k^* & (5c) \\ V_{af}[k] - \frac{V_2}{\sqrt{2}}, & \text{if } k^* < k < (k^* + w) & (5d) \\ 0, & \text{if } k \geq (k^* + w) & (5e) \end{cases}$$

where

$$V_{bf}[k] = \sqrt{\frac{1}{w} \left(\sum_{p=k}^{k^*-1} v_1[p]^2 + \sum_{p=k^*}^{k+w-1} v_2[p]^2 \right)} \quad (6)$$

$$V_{af}[k] = \sqrt{\frac{1}{w} \left(\sum_{p=k-w}^{k^*-1} v_1[p]^2 + \sum_{p=k^*}^{k-1} v_2[p]^2 \right)}$$

Note that $V_{rms}^{diff}[k] = V_{rms}^{past}[k] - V_{rms}^{future}[k]$ in (5) because $V_2 < V_1$ (sag), i.e., the V_{rms}^{future} value decreases after the inception instant. The relation is reversed for a voltage swell, i.e., $V_{rms}^{diff}[k] = V_{rms}^{future}[k] - V_{rms}^{past}[k]$. Considering the quantities defined in (6), where $V_2 < V_1$, results in:

$$V_{bf}[k] > \left(\sqrt{\frac{1}{w} \sum_{p=k}^{k+w-1} v_2[p]^2} = \frac{V_2}{\sqrt{2}} \right) \quad (7)$$

$$V_{af}[k] < \left(\sqrt{\frac{1}{w} \sum_{p=k-w}^{k-1} v_1[p]^2} = \frac{V_1}{\sqrt{2}} \right) \quad (8)$$

Substitution of (7) and (8) into (5b) and (5d), respectively, shows that V_{rms}^{diff} is maximum at the inception instant k^* , as represented in (9).

$$\begin{aligned} \left(V_{rms}^{diff}[k] = \frac{V_1}{\sqrt{2}} - V_{bf}[k] \right) &< \left(\frac{V_1 - V_2}{\sqrt{2}} = V_{rms}^{diff}[k^*] \right) \\ \left(V_{rms}^{diff}[k] = V_{af}[k] - \frac{V_2}{\sqrt{2}} \right) &< \left(\frac{V_1 - V_2}{\sqrt{2}} = V_{rms}^{diff}[k^*] \right) \end{aligned} \quad (9)$$

Therefore, $V_{rms}^{diff}[k^*]$ is a local maximum, as initially assumed. The same result is obtained for a voltage swell.

This concept is exemplified in Fig. 4a, which corresponds to a simulated voltage waveform with magnitudes 1, 0.01, 0.025, and 0.008 pu for the fundamental, 3rd, 5th, and 7th harmonics, respectively. A Gaussian noise between -0.005 and 0.005 pu is superimposed to the signal, and a 0.3 pu voltage sag is applied between 0.1 s and 0.15 s. As an example, four points in proximity of the sag inception instant are analyzed, adopting $w = 1$ cycle. The resulting V_{rms}^{diff} profile is shown in Fig. 4f:

- (k_1) full pre-sag inception instant (Fig. 4b): both *past* and *future* windows contain exclusively pre-sag voltage samples. In this case, V_{rms}^{diff} is quite small and the non-zero values are due to the normal voltage fluctuations experienced by the grid;
- (k_2) partial pre-sag inception instant (Fig. 4c): the *past* window contains exclusively pre-sag voltage samples, while the *future* window contains both pre- and during-sag voltage samples. Therefore, V_{rms}^{future} value decreases and V_{rms}^{diff} increases compared to (k_1);
- (k_3) sag inception instant (Fig. 4d): the *past* and *future* windows contain exclusively pre- and during-sag voltage samples, respectively. Thus, V_{rms}^{diff} is maximum;
- (k_4) partial post-sag inception instant (Fig. 4e): the *future* window contains exclusively during-sag voltage samples, while the *past* window contains both pre- and during-sag voltage samples. Therefore, both V_{rms}^{past} and V_{rms}^{diff} values decrease compared to (k_3).

The analysis regarding the sag recovery instant is analogous, corresponding to the second local maximum in Fig. 4f.

B. Determination of Inception and Recovery Instants

The procedure to determine the inception and recovery instants of a voltage sag is explained below. The starting point is the computation of the traditional rms voltage profile, as defined in (1). A voltage sag is detected if any computed rms value is lower than the threshold setting, α_{inf} ; the initial approximation for the inception point, k_{inc} , is the first instant where (10) is satisfied.

$$V_{rms}[k_{inc}] < \alpha_{inf} \quad (10)$$

As discussed in Section II, the traditional threshold rms voltage method has a time latency of up to 1 cycle (the length of the transition segment) in determining inception and recovery instants. Therefore, in the proposed method, the V_{rms}^{past} and V_{rms}^{future} profiles are computed for all indices ranging from $(k_{inc} - N)$ to k_{inc} . The revised and more accurate inception point, k_{inc}^* , is set to the index where V_{rms}^{diff} is maximum in this range.

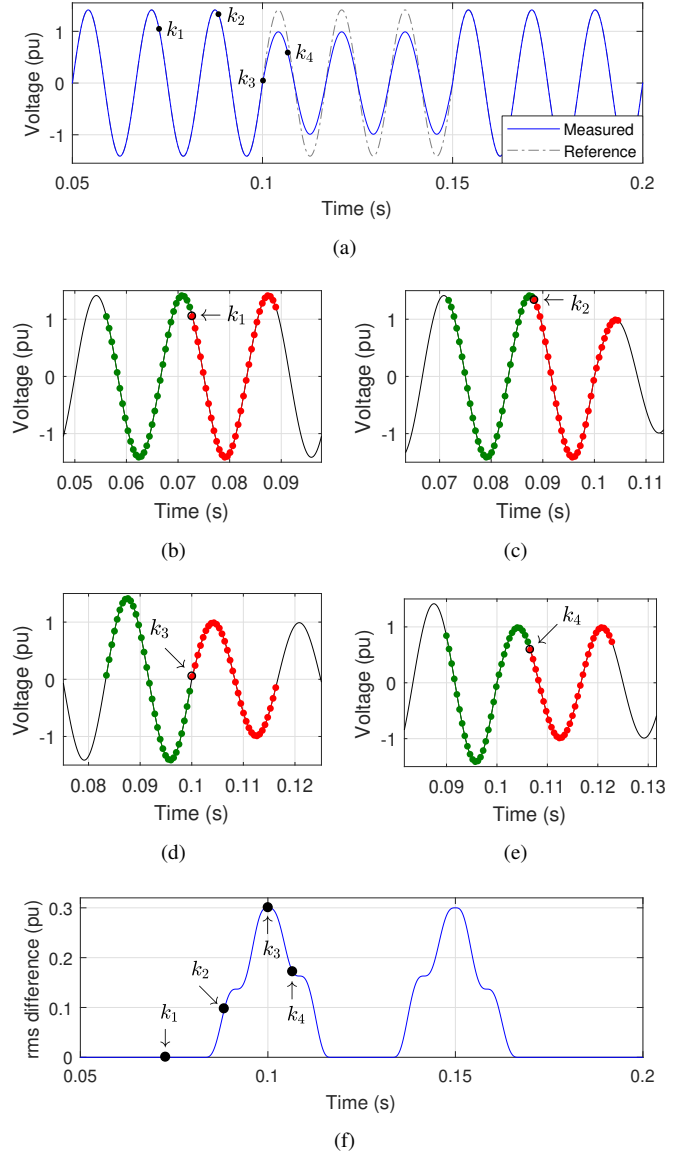


Fig. 4. Illustration of the rms voltage difference estimation method for a simulated sag. (a) Voltage waveform. (b) Pre-sag (*past* window: green dots, *future* window: red dots). (c) Transition before inception. (d) Sag inception. (e) Transition after inception. (f) V_{rms}^{diff} profile.

The initial estimate for the recovery point, k_{rec} , is the first instant that satisfies (11), i.e., the first instant after the sag inception where the voltage waveform has recovered above the minimum threshold for at least half-cycle. The revised estimate for the recovery point, k_{rec}^* , is computed similarly to k_{inc}^* , considering the index range from $(k_{rec} - N)$ to k_{rec} .

$$\begin{aligned} k_{rec} > k_{inc} \\ \min(V_{rms}[k_{rec} : k_{rec} + N/2 - 1]) > \alpha_{inf} \end{aligned} \quad (11)$$

The evolving instants of a multiple-stage sag are also identified. Once the inception and recovery instants have been determined, a V_{rms}^{diff} value larger than α_{evolve} for the time indices between $(k_{inc}^* + w)$ and $(k_{rec}^* - w)$ is assumed to represent a new stage of the sag. The inception instant of the new stage, k_{evolve}^* , is determined similarly to k_{inc}^* . Note that the choice for α_{evolve} is arbitrary; setting it equal to

$(1 - \alpha_{inf})/2$ (half of the minimum magnitude of a voltage sag/swell) seems reasonable.

Once the inception, recovery, and possibly evolving instants have been determined, an adjusted rms voltage profile, V_{rms}^{adj} , is computed to characterize the voltage variation event, such that the slow rms transitions around inception and recovery instants are eliminated. Using the traditional rms profile definition in (1), the rms profile transitions occur for the indices from k_{inc}^* to $(k_{inc}^* + w)$ and from k_{rec}^* to $(k_{rec}^* + w)$; therefore, $V_{rms}^{adj} = V_{rms}^{future}$ in those ranges, since the *future* rms values are computed using exclusively during- or post- voltage samples, respectively. For all other time indices, $V_{rms}^{adj} = V_{rms}^{past}$. The piecewise definition of the V_{rms}^{adj} profile is presented in (12); for simplicity, it is assumed that the event does not contain multiple stages. If this is not the case, the corresponding additional stages are introduced between $(k_{inc}^* + w + 1)$ and $(k_{rec}^* - 1)$ in a similar manner.

$$V_{rms}^{adj}[k] = \begin{cases} V_{rms}^{future}[k], & \text{if } k_{inc}^* \leq k \leq (k_{inc}^* + w) \\ & \text{or } k_{rec}^* \leq k \leq (k_{rec}^* + w) \\ V_{rms}^{past}[k], & \text{otherwise} \end{cases} \quad (12)$$

The rms voltage difference method is also suitable for determining the inception and recovery instants of a voltage swell. The following adjustments are needed: the input α_{inf} must be replaced by α_{sup} , the threshold setting for swell detection; and the conditions in (10) and (11) become $V_{rms}[k_{inc}] > \alpha_{sup}$ and $\max(V_{rms}[k_{rec} : k_{rec} + N/2 - 1]) < \alpha_{sup}$, respectively.

IV. PERFORMANCE ASSESSMENT

The performance of the rms voltage difference method is assessed for different sets of measured voltage sags and swells. These rms voltage variation events were obtained from field data recorded at the substation transformer of a 25-kV, 60 Hz distribution system with multiple parallel feeders. The instantaneous phase-to-neutral voltage waveforms are sampled at the frequency of 7.68 kHz. The values $\alpha_{inf} = 0.9$ pu and $\alpha_{sup} = 1.1$ pu are adopted as thresholds for sag and swell detection, respectively, and $w = 128$ samples (1 cycle) is chosen for the sliding window length, unless stated otherwise.

For each rms voltage variation event, its estimated duration and time latency for the inception and recovery instants are reported. Whenever possible, the exact values for these parameters are determined by visual inspection of the voltage waveforms. The error in the estimated event duration, in %, is computed according to (13).

$$d_{error} = \frac{d_{estimated} - d_{exact}}{d_{exact}} \times 100\% \quad (13)$$

where d_{exact} and $d_{estimated}$ are the exact and estimated duration of the event, respectively.

A. Voltage Sag Accompanied by Transients

Voltage variation events are commonly accompanied by transients during inception and recovery, as for the case of the voltage sag represented in Fig. 5a. The exact event duration is estimated to be 1.984 cycles by visual inspection of the voltage waveform. Fig. 5b illustrates the application of the proposed

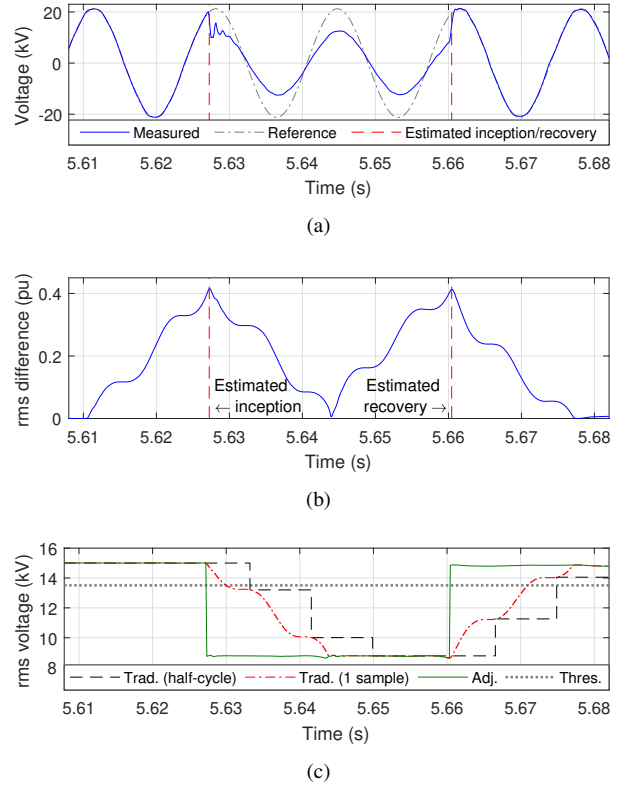


Fig. 5. Voltage sag accompanied by transients. (a) Voltage waveform. (b) V_{rms}^{diff} profile and the corresponding inception and recovery instants. (c) Traditional (half-cycle and 1 sample update) and adjusted rms voltage profiles.

TABLE I
TIME LATENCY OF THE TRADITIONAL AND PROPOSED METHODS FOR A VOLTAGE SAG ACCOMPANIED BY TRANSIENTS

Method	Latency (samples)		Duration* (cycle)	d_{error} (%)
	Inception	Recovery		
Traditional 1 ^(a)	46	112	2.500	+26.01
Traditional 2 ^(b)	21	82	2.461	+24.04
rms voltage difference	0	1	1.992	+0.40

^(a) rms update rate: half-cycle ^(b) rms update rate: 1 sample

* Exact duration: 1.984 cycles

method; the peaks of V_{rms}^{diff} correspond to the estimated inception and recovery instants, which have a time latency of 0 and 1 sample in relation to the exact instants, respectively. On the contrary, Fig. 5c illustrates that when the traditional method is used, there is a significant delay in the estimate of the inception and recovery instants, in spite of the rms update rate. This can be verified by inspection: both the black dashed and the red dashed-dotted lines cross the threshold with a visible delay compared to the proposed method.

As shown in Table I, the time latency in the traditional method is as high as 112 samples (0.875 cycle) and the event duration is overestimated by up to 26.01%. The proposed method, on the contrary, introduces negligible time latency.

B. Voltage Sag Not Accompanied by Transients

Sags not accompanied by transients compose the next class of voltage variation events analyzed. In these events, the transient in the voltage waveform during the transition from pre-

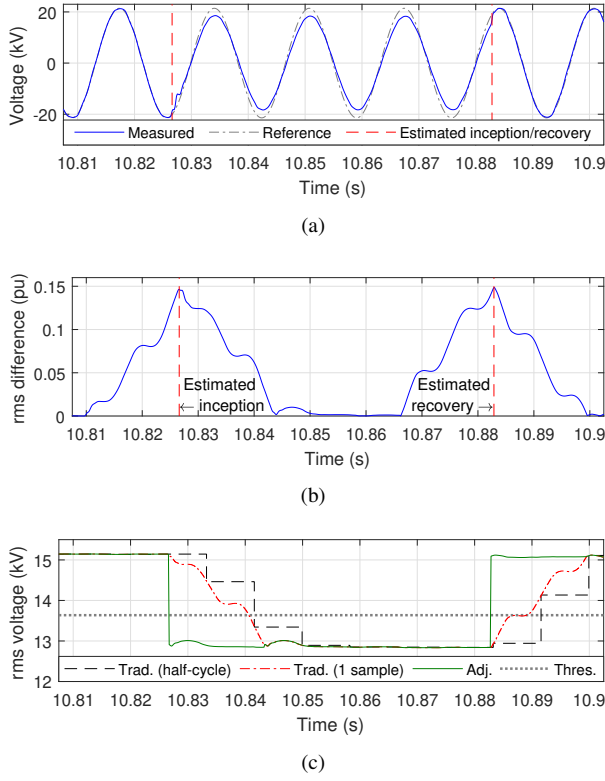


Fig. 6. Voltage sag not accompanied by transients. (a) Voltage waveform. (b) V_{rms}^{diff} profile and the corresponding inception and recovery instants. (c) Traditional (half-cycle and 1 sample update) and adjusted rms voltage profiles.

TABLE II

TIME LATENCY OF THE TRADITIONAL AND PROPOSED METHODS FOR A VOLTAGE SAG NOT ACCOMPANIED BY TRANSIENTS

Method	Latency (samples)		Duration* (cycle)	d_{error} (%)
	Inception	Recovery		
Traditional 1 (a)	116	68	3.000	-11.11
Traditional 2 (b)	109	48	2.898	-14.13
rms voltage difference	1	1	3.375	0.00

(a) rms update rate: half-cycle (b) rms update rate: 1 sample

* Exact duration: 3.375 cycles

to during-sag and from during- to post-sag are non-existent or very subtle. Fig. 6a depicts an example of a sag pertaining to this class of events. Although it is still possible to estimate the inception and recovery instants by visually inspecting the voltage waveform, automating this process through the techniques found in the literature is challenging [22].

The rms voltage difference method is able to accurately determine the inception and recovery instants for this voltage sag, regardless of the presence of transient components. For the example shown in Fig. 6, the time latency is 1 sample for both inception and recovery points estimated by the proposed method, while it is higher than 0.9 cycle for the traditional method (see Table II).

Unlike the example of a voltage sag with transients presented in Fig. 5, the traditional method underestimates the event duration in this case. There is no general rule to predict whether the event duration calculated by the traditional method will be an underestimation or overestimation in relation to the

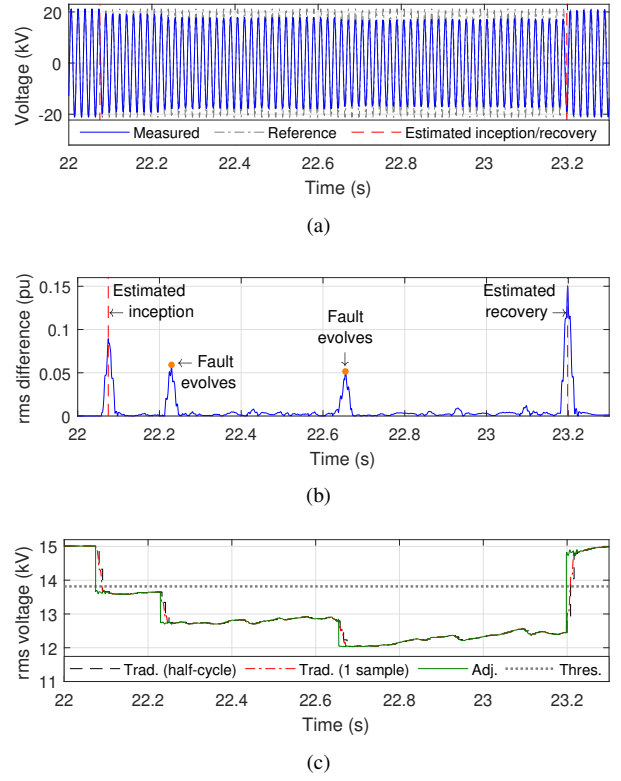


Fig. 7. Voltage sag with multiple stages. (a) Voltage waveform. (b) V_{rms}^{diff} profile and the corresponding inception and recovery instants. (c) Traditional (half-cycle and 1 sample update) and adjusted rms voltage profiles.

exact value. This estimate depends on the points on waveform at which rms values are updated, as discussed in Section II.

C. Voltage Sag with Multiple Stages

A voltage sag may contain multiple stages, such that the voltage level changes in steps during the event. For example, Fig. 7a depicts a voltage sag with three stages. The inception and recovery instants are accurately determined by applying the rms voltage difference method, as in the previous examples. Estimating the evolving instants, however, is subject to the choice of α_{evolve} , the threshold value for detection of evolving sags. Industry standards [1], [2] offer no recommendation for this value, and an improper choice may result in either over-detection (α_{evolve} is too small) or under-detection (α_{evolve} is too large). For this example, $\alpha_{evolve} = (1 - \alpha_{inf})/2 = 0.05$ pu is appropriate.

Fig. 7b shows that inception, recovery, and evolving instants are accurately estimated by the rms voltage difference method. On the other hand, Fig. 7c shows that the traditional method is not able to identify the evolving instants.

As already discussed, the proposed method inhibits the detection of the evolving instants if they are located less than w samples from each other. This constraint is used to guarantee the accuracy of the estimated instants. For example, suppose that the fault evolves to a new stage at $(k_{inc}^* + w/2)$. At this instant, V_{rms}^{past} is still affected by the pre-sag voltage values, and it cannot be guaranteed that V_{rms}^{diff} has reached its maximum value. Using shorter sliding windows alleviates

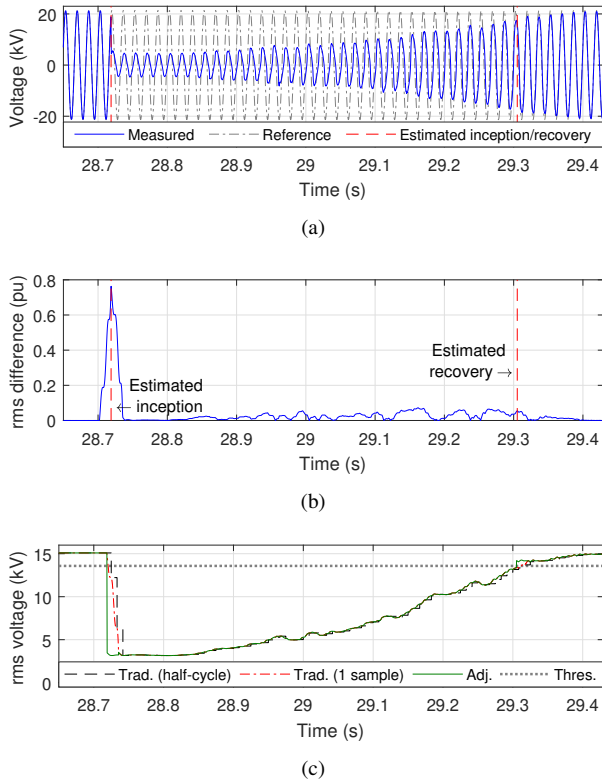


Fig. 8. Voltage sag followed by slow recovery. (a) Voltage waveform. (b) V_{rms}^{diff} profile and the corresponding inception and recovery instants. (c) Traditional (half-cycle and 1 sample update) and adjusted rms voltage profiles.

TABLE III

TIME LATENCY OF THE TRADITIONAL AND PROPOSED METHODS FOR A VOLTAGE SAG FOLLOWED BY SLOW RECOVERY

Method	Latency (samples)		Duration (cycle)
	Inception	Recovery	
Traditional 1 ^(a)	98	<i>n/a</i>	35.500
Traditional 2 ^(b)	29	<i>n/a</i>	35.512
rms voltage difference	3	<i>n/a</i>	35.184

^(a) rms update rate: half-cycle ^(b) rms update rate: 1 sample

this limitation; an analysis of the effect of the sliding window length is presented in Section IV-F.

D. Voltage Sag Followed by Slow Recovery

Not all voltage variation events present well-defined time boundaries. The voltage sag caused by the starting of a large motor is a case in which the voltage drops substantially at the event inception, then gradually recovers to its pre-sag value. The voltage sag represented in Fig. 8a is an example of such behavior (this voltage waveform is sampled at 15.36 kHz, i.e., 256 samples/cycle). Note that the sag recovery instant cannot be determined by visually inspecting the voltage waveform; therefore, it is not possible to calculate the time latency introduced by each method in estimating the recovery instant.

The rms voltage variation events caused by faults present a well-defined point-on-wave recovery instant that corresponds to the operation instant of the protective device (fuses, reclosers). On the other hand, the voltage waveforms of events

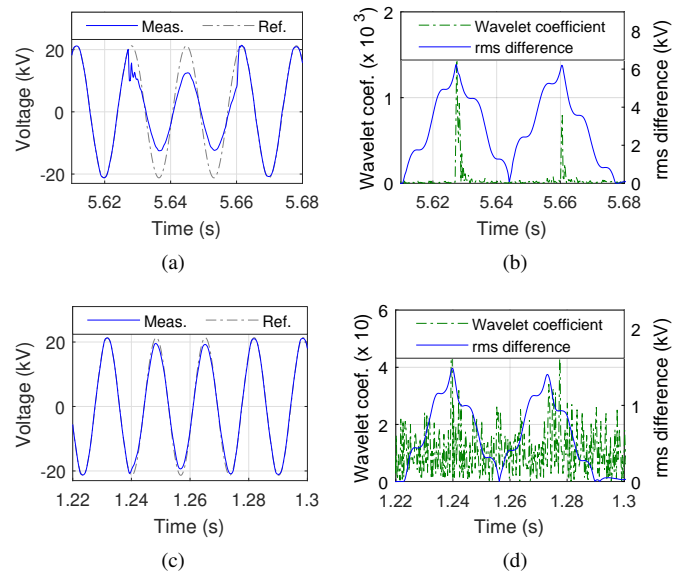


Fig. 9. Comparison of the rms voltage difference and DWT methods. (a)-(b) Sag with transients. (c)-(d) Sag without transients.

with a slow recovery do not contain a real point-on-wave recovery instant [8], since the underlying power system event (such as motor starting or similar large load energizing) is not cleared by protective devices.

As shown in Table III, the resulting inception instants are similar to the previous examples: the proposed method introduces a time latency of only three samples, while the traditional threshold rms voltage method introduces significantly large time latency. On the other hand, the rms voltage difference method performs no better than the traditional method in estimating the recovery instant. According to the conditions presented in (11), the proposed method initially computes the recovery instant based on the traditional method, obtaining k_{rec} . Then, this first approximation is improved through the analysis of the V_{rms}^{diff} profile around k_{rec} . However, due to the gradual voltage recovery, the portion of the V_{rms}^{diff} profile under analysis contains no noticeable local maximum (refer to Fig. 8b), and the recovery instant estimate is not improved.

E. Comparison to the Discrete Wavelet Transform Method

A previous survey indicated that the discrete wavelet transform (DWT) presents the best performance among the methods for determining the inception and recovery points of a voltage sag [22]. Fig. 9 compares the rms voltage difference and DWT estimation methods under two scenarios: voltage sag with and without transients. The DWT method uses *db6* as mother wavelet [9].

Both the DWT and the rms voltage difference methods are equally accurate in determining the inception and recovery instants of a voltage sag accompanied by transients, and the estimated instants are exactly the same in this example, as shown in Fig. 9a and 9b. On the other hand, when the voltage sag is not accompanied by transients, the inception and recovery instants are undetected by the DWT method, while they are accurately determined by the rms voltage difference method (see Fig. 9c and 9d). The wavelet coefficients rise

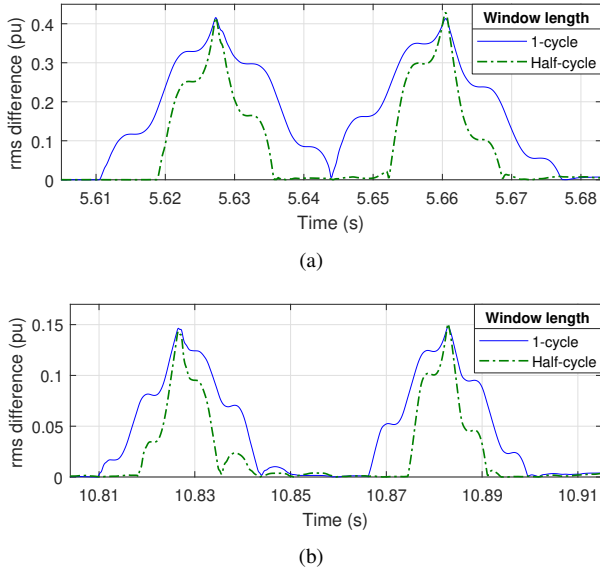


Fig. 10. V_{rms}^{diff} profile obtained through 1-cycle and half-cycle long sliding windows. (a) Sag with transients. (b) Sag without transients.

slightly around the inception and recovery instants; however, such increase is not sufficient to detect them as outliers.

The accuracy and false-negative rate of the DWT method is highly dependent on the mother wavelet choice, while the rms voltage difference method does not have this shortcoming. Furthermore, the DWT method provides no information about the retained voltage during the event, and it is prone to overdetection, as any transient event has the potential to affect the wavelet coefficients [26].

F. Effect of the Sliding Window Length

The previous examples use $w = 128$ samples, i.e., the sliding window length is 1 cycle, as in the traditional method. The effect of decreasing this value to half-cycle is analyzed in Fig. 10, where the V_{rms}^{diff} profiles in (a) and (b) are obtained from the voltage sags discussed in Sections IV-A and IV-B, respectively, for two different values of the window length.

Reducing the window length did not affect the time latency introduced by the rms voltage difference method in these examples. The estimated inception and recovery instants are the same for both 1-cycle and half-cycle long sliding windows, regardless of the presence of transients. However, as the peaks in V_{rms}^{diff} get sharper for half-cycle windows, it has the potential to decrease the time latency.

The half-cycle rms computation provides a faster transition between event and non-event values, as can be observed by the narrower interval where V_{rms}^{diff} is considerably large. Assume that a voltage sag starts at k_{inc}^* ; then the V_{rms}^{diff} values for indices from $(k_{inc}^* - N)$ to $(k_{inc}^* + N)$ are affected by the voltage sag values for the 1-cycle window case, while this range is reduced to $(k_{inc}^* - N/2)$ to $(k_{inc}^* + N/2)$ for the half-cycle window case. The minimum duration of a voltage sag detected in each case is 1 cycle and half-cycle, respectively.

On the other hand, half-cycle rms computation is sensitive to even-harmonic distortion [7]. In such cases, consecutive half-cycles of the voltage waveform do not present odd symme-

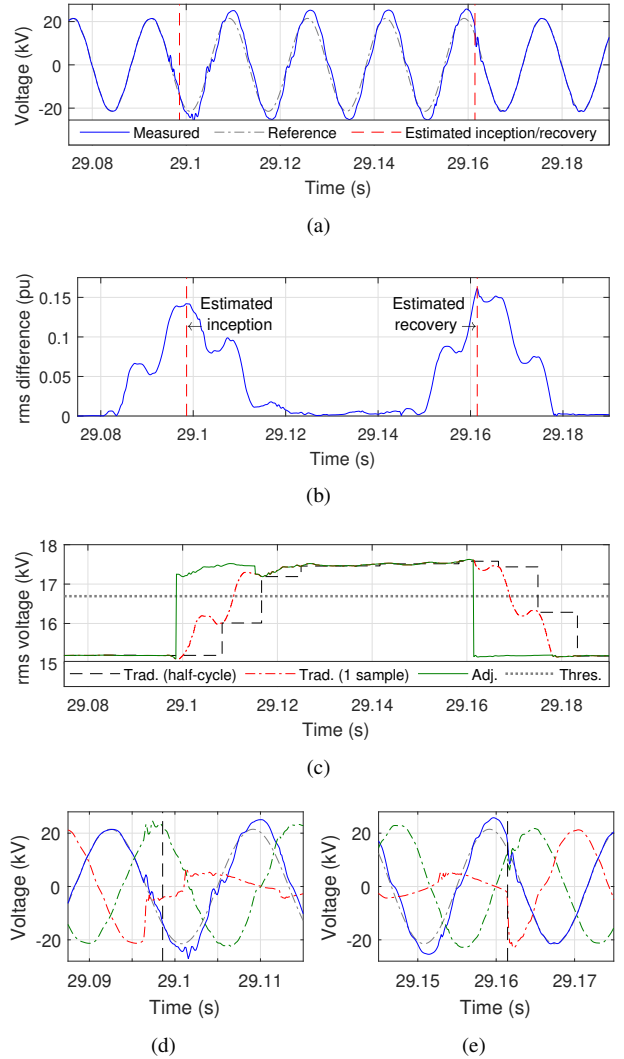


Fig. 11. Voltage swell. (a) Voltage waveform. (b) V_{rms}^{diff} profile and the corresponding inception and recovery instants. (c) Traditional (half-cycle and 1 sample update) and adjusted rms voltage profiles. (d) Zoom-in at inception. (e) Zoom-in at recovery.

try, and the rms voltage profile varies significantly between consecutive computations. Examples of events with even-harmonic distortion include voltage sags due to transformer energizing and sags associated with post-fault transformer saturation [7].

Therefore, it is recommended to use shorter sliding windows ($w = \text{half-cycle}$), unless high levels of even-harmonic distortion are anticipated. The choice of the window length can be performed automatically, by setting the default value to half-cycle, which is increased to $w = \text{one-cycle}$ when the even-harmonic distortion is above a certain threshold value.

G. Voltage Swell Accompanied by Transients

The previous examples illustrated the performance of the proposed method in determining the inception and recovery instants of voltage sags. This method is also applicable to voltage swells if (10) and (11) are modified accordingly, as discussed in Section III. Fig. 11a represents a voltage swell, and the respective estimated inception and recovery instants.

This voltage waveform corresponds to a healthy phase during a single line-to-ground fault; the faulted phase is represented in red in Fig. 11d and 11e.

It is worth noting that there is a voltage transient preceding the estimated inception instant. However, the time interval between the transient start and the estimated inception should not be considered as time latency for the proposed method. Upon closer inspection, the transient in the healthy phase is due to the fault in one of the other phases. The comparison between the measured and reference waveforms shows that the swell does not start until the instant labeled as *estimated inception*, as shown in Fig. 11d. Therefore, the inception instant is accurately determined by the proposed method. The same reasoning applies to the estimated recovery instant.

V. CONCLUSION

This paper presents a robust method based on rms voltage differences to accurately determine the inception and recovery instants of voltage variation events. The largest time latency observed was three samples, which corresponds to a deviation of only 4.22° in estimating the point-on-wave. The traditional method, on the contrary, had a time latency up to 116 samples. It is recommended to use short sliding windows (half-cycle), which allows identification of events as short as half-cycle, while longer sliding windows can be used when even harmonic distortion is above a pre-determined level. In the unlikely event of high voltage distortion, a low-pass filter may be necessary prior to the identification of the inception and recovery instants. The main application of the proposed method is to obtain accurate statistics on point-on-wave instants for equipment sensitivity analysis.

REFERENCES

- [1] *IEEE Guide for Voltage Sag Indices*, IEEE Std. 1564-2014, March 2014.
- [2] *IEC Electromagnetic Compatibility: Testing and measurements techniques - Power quality measurement methods*, IEC 61000-4-30, 2015.
- [3] *IEEE Recommended Practice for Evaluating Electric Power System Compatibility with Electronic Process Equipment*, IEEE Std. 1346-1998, May 1998.
- [4] *IEC Electromagnetic Compatibility: Environment - Voltage dips and short interruptions of the electricity supplied by public distribution systems with statistical measurement results*, IEC 61000-2-8, 2002.
- [5] S. Djokic, J. Milanovic, and S. Rowland, "Advanced voltage sag characterization II: point-on-wave," *IET Gen., Trasm., and Distrib.*, vol. 1, no. 1, pp. 146–154, January 2007.
- [6] J. Barros and E. Perez, "Limitations in the use of rms value in power quality analysis," in *Proc. IEEE Instrumentation and Measurement Technical Conf.*, 2006, pp. 2261–2264.
- [7] M. Bollen and I. Gu, *Signal Processing of Power Quality Disturbances*. Hoboken, NJ: Wiley, 2006.
- [8] Y. Wang, X. Xiao, and M. Bollen, "Challenges in the calculation methods of point-on-wave characteristics for voltage dips," in *Proc. Int. Conf. on Harmonics and Quality of Power*, 2016.
- [9] A. C. Parsons, W. M. Grady, and E. J. Powers, "A wavelet-based procedure for automatically determining the beginning and end of transmission system voltage sags," in *Proc. IEEE Power and Energy Society General Meeting*, 1999.
- [10] E. Perez and J. Barros, "A proposal for on-line detection and classification of voltage events in power systems," *IEEE Trans. on Power Del.*, vol. 23, no. 4, pp. 2132–2138, October 2008.
- [11] F. Costa and J. Driesen, "Assessment of voltage sag indices based on scaling and wavelet coefficient energy analysis," *IEEE Trans. on Power Del.*, vol. 28, no. 1, pp. 336–346, January 2013.
- [12] O. Gencer, S. Ozturk, and T. Erfidan, "A new approach to voltage sag detection based on wavelet transform," *Int. J. Elect. Power and Energy Syst.*, vol. 32, no. 2, pp. 133–140, 2010.
- [13] M. Latran and A. Teke, "A novel wavelet transform based voltage sag/swell detection algorithm," *Int. J. Elect. Power and Energy Syst.*, vol. 71, pp. 131–139, 2015.
- [14] X. Yan, Q. Zhang, H. Liu, H. Zhao, and L. Li, "A method for rapid detection of the grid sudden change," in *Proc. IEEE Int. Conf. Sustainable Energy Tech.*, 2012.
- [15] Y. Cui, A. Sayed-Ahmed, P. Vadavkar, B. Seibel, and R. Kerkman, "A new instantaneous point-on-wave voltage sag detection algorithm and validation," in *Proc. IEEE Energy Conversion Cong. and Exp.*, 2016.
- [16] N. Tunaboylu, E. Collins, and P. Chaney, "Voltage disturbance evaluation using the missing voltage technique," in *Proc. Int. Conf. on Harmonics and Quality of Power*, 1998, pp. 577–582.
- [17] Z. Fan and X. Liu, "A novel universal grid voltage sag detection algorithm," in *Proc. IEEE Power Eng. and Automation Conf.*, 2012.
- [18] C. Fitzer, M. Barnes, and P. Green, "Voltage sag detection technique for a dynamic voltage restorer," *IEEE Trans. Ind. Appl.*, vol. 40, no. 1, pp. 203–212, Feb. 2004.
- [19] H. Chu, H. Jou, and C. Huang, "Transient response of a peak voltage detector for sinusoidal signals," *IEEE Trans. Ind. Electron.*, vol. 39, no. 1, pp. 74–79, Feb. 1992.
- [20] K. Ding, K. Cheng, X. Xue, B. Divakar, C. Xu, Y. Che, D. Wang, and P. Dong, "A novel detection method for voltage sags," in *Proc. Int. Conf. on Power Electronics Syst. and Appl.*, 2006, pp. 250–255.
- [21] W. Lee and T. Lee, "Peak detection method using two-delta operation for single voltage sag," in *Proc. Int. Power Elec. Conf.*, 2014, pp. 595–600.
- [22] A. F. Bastos, S. Santoso, and G. Todeschini, "Comparison of methods for determining inception and recovery points of voltage variation events," in *Proc. IEEE Power and Energy Society General Meeting*, 2018.
- [23] *IEEE Recommended Practice for Monitoring Electric Power Quality*, IEEE Std. 1159-2009, June 2009.
- [24] I. M. M. Garcia, A. M. Munoz, A. G. Castro, M. Bollen, and I. Y. H. Gu, "Novel segmentation technique for measured three-phase voltage dips," *Energies*, vol. 8, no. 8, pp. 8319–8338, August 2015.
- [25] C. D. Le, I. Y. H. Gu, and M. H. J. Bollen, "Joint causal and anti-causal segmentation and location of transitions in power disturbances," in *Proc. IEEE Power and Energy Society General Meeting*, July 2010, pp. 1–6.
- [26] A. F. Bastos and S. Santoso, "Identifying switched capacitor relative locations and energizing operations," in *Proc. IEEE Power and Energy Society General Meeting*, 2016.

Alvaro Furlani Bastos (S'15) received his B.Sc. degree in Electrical Engineering from the Federal University of Viçosa, Viçosa, Brazil, in 2014, and his M.Sc. degree in Electrical and Computer Engineering from The University of Texas at Austin in 2015, where he is currently pursuing his Ph.D. degree. His research interests include power quality and data analytics.

Keng-Weng Lao (S'09-M'17) received the B.Sc., M.Sc., and Ph.D. degrees in Electrical and Electronics Engineering from the Faculty of Science and Technology, University of Macau, Macao, in 2009, 2011, and 2016, respectively. He is currently a lecturer in the Department of Electrical and Computer Engineering at University of Macau. He is now also as a research scholar in the Department of Electrical and Computer Engineering at The University of Texas at Austin. His research interests include power quality compensation, renewable energy integration, energy saving and power system.

Grazia Todeschini (SM'14) received her B.Sc. and M.Sc. in Electrical Engineering from the Politecnico di Milano, Italy, and her Ph.D. in Electrical and Computer Engineering from Worcester Polytechnic Institute in Massachusetts. She was Senior Consultant with EnerNex in Knoxville from 2010 to 2013, and Senior Power Studies Engineer with General Electric in Philadelphia from 2013 to 2016. She became Senior Lecturer at Swansea University, UK, in 2016. Her research interests include power quality, renewable energy integration, and power system analysis.

Surya Santoso (F'15) earned his B.S. degree from Satya Wacana Christian University, Salatiga, Indonesia, in 1992, and M.S.E. and Ph.D. degrees in Electrical and Computer Engineering from The University of Texas at Austin, in 1994 and 1996, respectively. He was a Senior Power Systems and Consulting Engineer with Electrotek Concepts, Knoxville, TN, USA, from 1997 to 2003. He joined the faculty of The University of Texas at Austin in 2003 and is currently Professor of Electrical and Computer Engineering. His research interests include power quality, power systems, and renewable energy integration in transmission and distribution systems. He is co-author of *Electrical Power Systems Quality* (3rd edition), sole author of *Fundamentals of Electric Power Quality*, and editor of *Handbook of Electric Power Calculations* (4th edition) and *Standard Handbook for Electrical Engineers* (17th edition). He is an IEEE Fellow.